Electronic Supplementary Material (ESI) for Journal of Materials Chemistry C.

Supporting Information

High-performance Self-powered Photodetector Based on Concentric Annular α-$FAPbI_3$/$MAPbI_3$ Single Crystals Lateral Heterojunction with Broadband Detectivity

Hu Zhang [a], Zhiliang Chen *[abc], Yanhui Li [a], Jianfeng Yao [a], Duanwangde Liu [a], Wei Zeng [a], Pengbin Gui [a], Zhixiang Huang *[ac]

[a] Information Materials and Intelligent Sensing Laboratory of Anhui Province, Anhui University, No. 111 Jiulong Road, Hefei, Anhui Province, People's Republic of China.

[b] Anhui Province Key Laboratory of Target Recognition and Feature Extraction, Lu'an, Anhui Province, People's Republic of China.

[c] Hefei Comprehensive National Science Center, Hefei 230601, Anhui, People's Republic of China

*Corresponding authors: Zhixiang Huang (zxhuang@ahu.edu.cn) and Zhiliang Chen (zhiliang.chen@ahu.edu.cn)

To obtain $FAPbI_3$ single crystals, a concentration of 1.2 M is chosen in present work, then the proper temperature range for crystal growth should be carefully considered. The solubility curve of $FAPbI_3$ in γ-GBL is tested as following figure. In order to obtain $FAPbI_3$ single crystals via inverse temperature crystallization, the temperature should be at least ~65°C. To obtain $FAPbI_3$ single crystal seeds in a shorter time, we choose 105°C for growth temperature of $FAPbI_3$ single crystal seeds. However, after obtaining $FAPbI_3$ single crystal seeds, the temperature should be lower than 105°C but higher than 65°C for subsequent quality $FAPbI_3$ single crystal wafer growth. In our work, we found the temperature values ranging from 75°C to 85°C is proper. For liquid phase epitaxy of $MAPbI_3$ single crystal, the same solvent (γ-GBL) and concentration (1.2 M) are chosen, while the temperature is ranging from 88°C to 95°C.

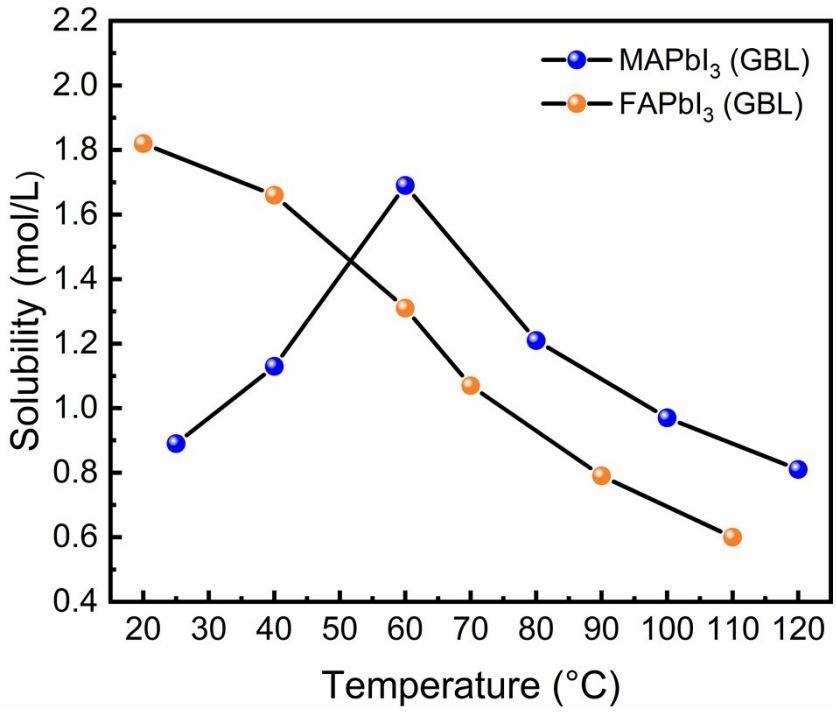

Fig. S1 The solubility of $FAPbI_3$ and $MAPbI_3$ in γ-GBL.

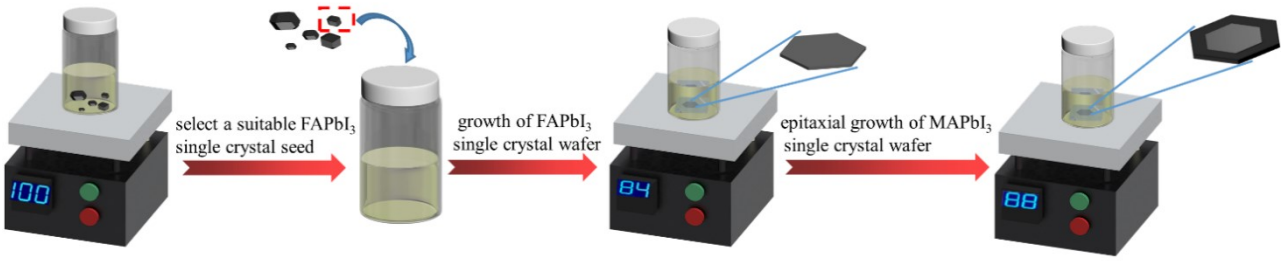

Fig. S2 Flow diagram of epitaxial growth of $FAPbI_3/MAPbI_3$ SCs concentric annular lateral heterojunction.

Fig. S3 Grow $FAPbI_3$ SC a) without using the seeds, the inset shows needle-like yellow δ-$FAPbI_3$ perovskites. b) using the seeds. c) using the SCITC method.

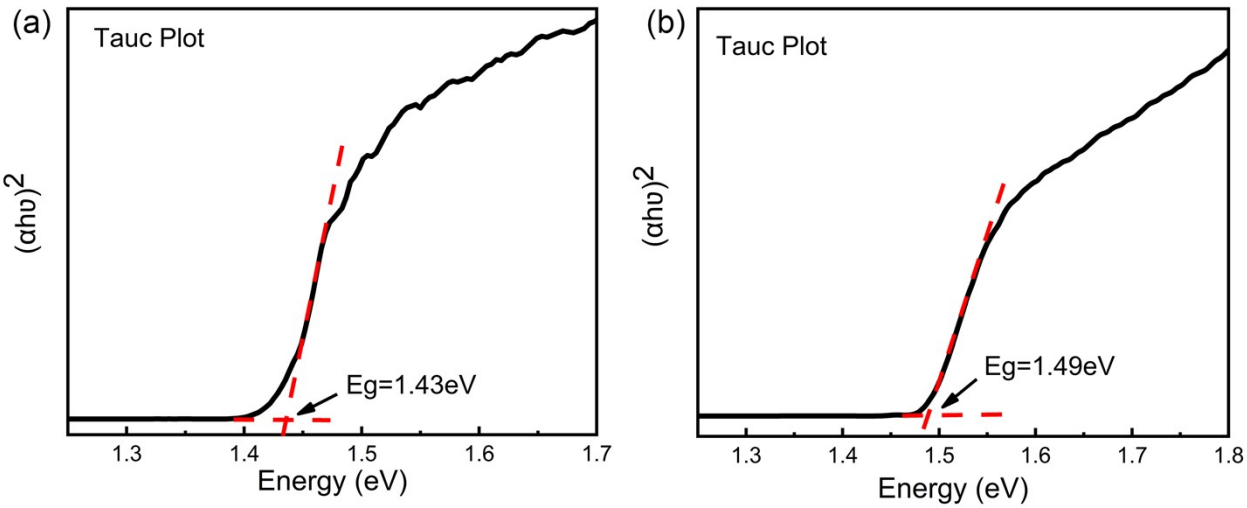

Fig. S4 Tauc plots of c) $FAPbI_3$ SC and d) $MAPbI_3$ SC obtained from their absorbance spectra.

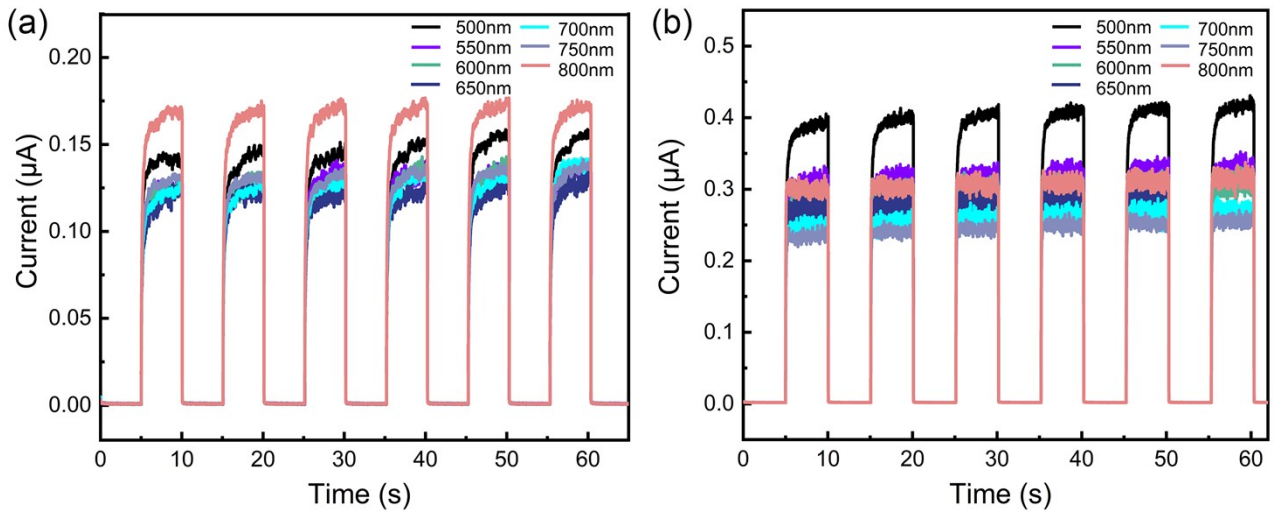

Fig. S5 Time-dependent photoresponse under light illumination (0.19 mW cm^{-2}) ranging from 500 nm to 800 nm at a) -1 V bias. b) -2 V bias.

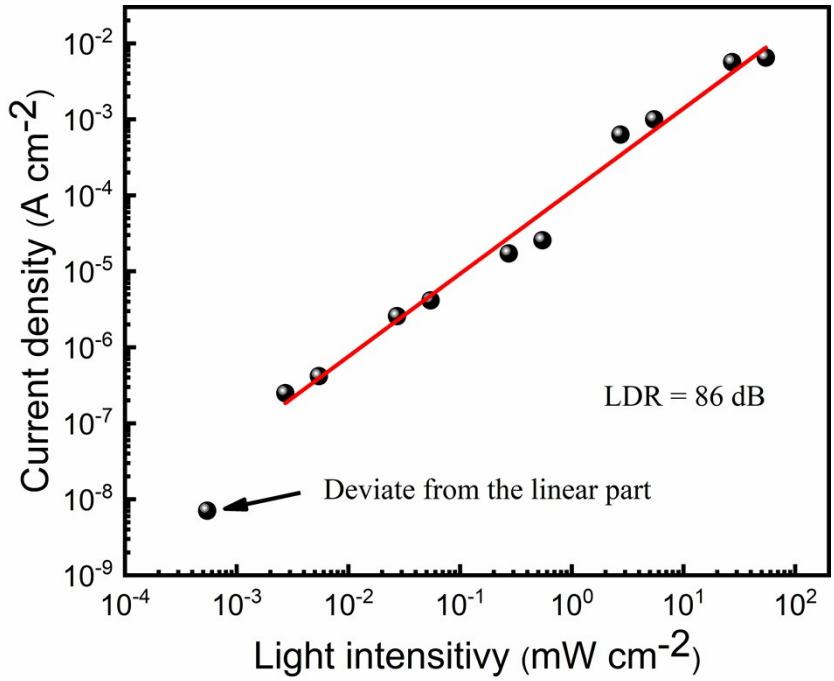

Fig. S6 LDR of the device tested under 530 nm illumination at a bias of -3 V.

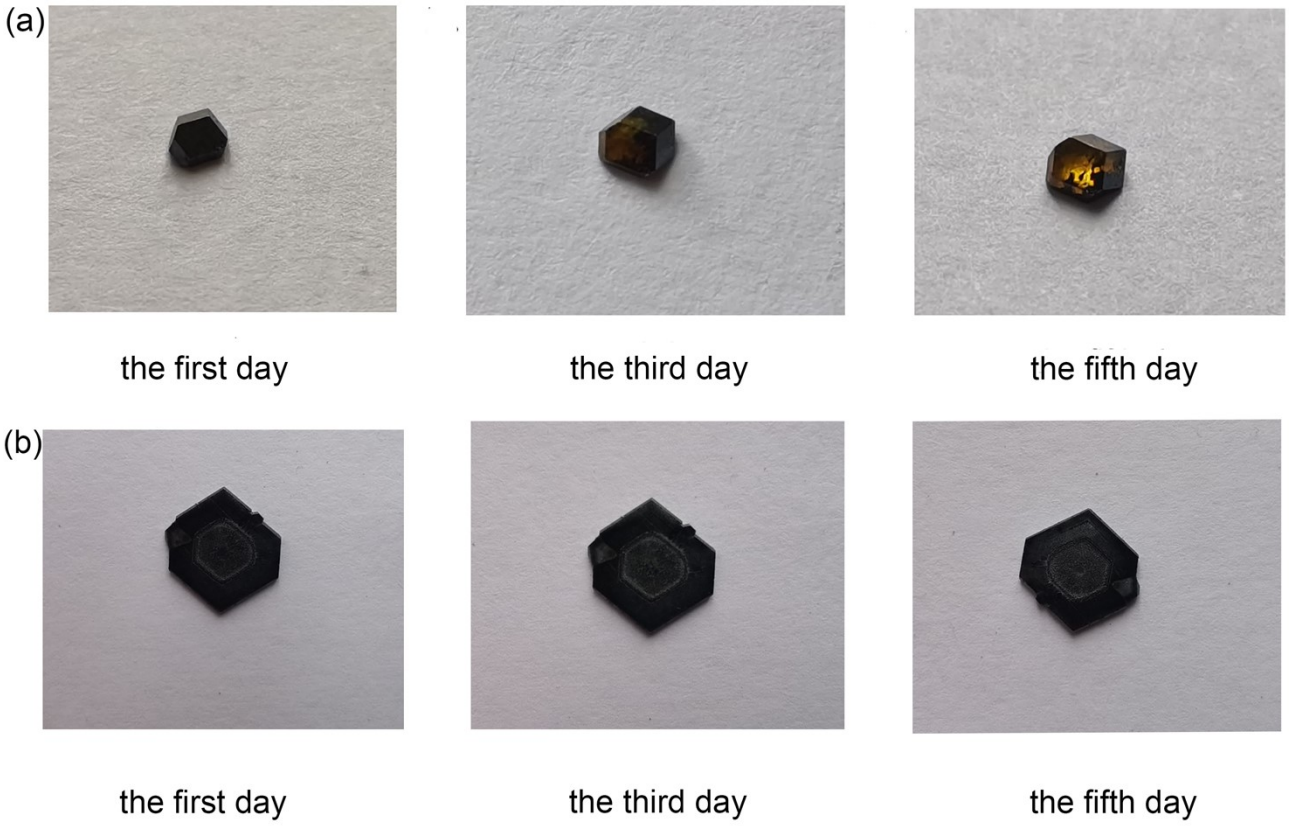

Fig. S7 Comparison of stability between pristine $FAPbI_3$ SC and α-$FAPbI_3$/$MAPbI_3$ SC lateral heterojunction.

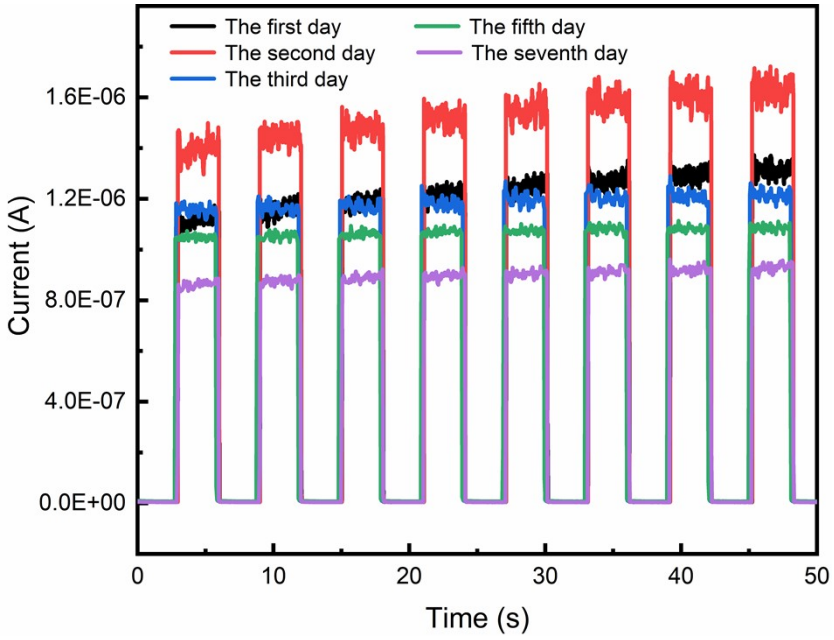

Fig. S8 The stability test of the unencapsulated device.

Table S1 Parameters of perovskites

Species	Lattice constant	Band gap	Crystal system
$FAPbI_3$	6.40 Å [1]	1.43 eV	cubic
$FAPbBr_3$	6.03 Å [2]	2.26 eV [3]	cubic
$FAPbCl_3$	6.2 Å [4]	2.84 eV [4]	cubic
$MAPbI_3$	6.276 Å [5]	1.49 eV	cubic
$MAPbBr_3$	5.872 Å [6]	2.3 eV [7]	cubic
$MAPbCl_3$	5.7 Å [8]	2.85 eV [9]	cubic
$CsPbI_3$	6.18 Å [10]	1.67 eV [11]	cubic
$CsPbBr_3$	5.87 Å [12]	2.25 eV [13]	cubic
$CsPbCl_3$	5.61 Å [14]	3.1 eV [15]	cubic

The lattice misfits can be calculated by the following formula:

f(epitaxial layer, substrate) = [a(epitaxial layer)-a(substrate)]/a(substrate)]

Where a(epitaxial layer) is the lattice constant of epitaxial layer, a(substrate) is the lattice constant of substrate, so the lattice misfits between different kinds of perovskites are calculated as follows:

$f(FAPbBr_3, FAPbI_3)$ =-5.78,

$f(FAPbCl_3, FAPbI_3)$ =-3.13,

$f(MAPbI_3, FAPbI_3)$ =-1.94,

$f(MAPbBr_3, FAPbI_3)$ =-8.25,

$f(MAPbCl_3, FAPbI_3)$ =-10.94,

$f(CsPbI_3, FAPbI_3)$ =-3.44,

$f(CsPbBr_3, FAPbI_3)$ =-8.28,

$f(CsPbCl_3, FAPbI_3)$ =-12.34,

$f(FAPbI_3, MAPbI_3)$ =1.98,

$f(FAPbBr_3, MAPbI_3)$ =-3.92,

$f(FAPbCl_3, MAPbI_3)$ =-1.21,

$f(MAPbBr_3, MAPbI_3)$ =-6.44,

f($MAPbCl_3$, $MAPbI_3$) =-9.18,

f($CsPbI_3$, $MAPbI_3$) =-1.53,

f($CsPbBr_3$, $MAPbI_3$) =-6.47,

f($CsPbCl_3$, $MAPbI_3$) =-10.61.

Table S2 Performance comparison of perovskite-based photodetectors

Material structure	Light wavelength (nm)/power	R (mA W^{-1})
$MAPbI_3$ microwires/Graphene	520 nm/13.5 mW cm^{-2}	2.2
$CsPbI_3$-$CsPbBr_3$ anowire Array	650 nm/0.5 μW cm^{-2}	125
$MAPbBr_3$/Graphene	532 nm/0.66 mW cm^{-2}	1.017×10^6
$CsPbBr_3$Monocrystalline Films	530 nm/216 μW cm^{-2}	_
$CsPbrB_3$/CuI	540 nm/216 μW cm^{-2}	1.4
$MAPbICl_2$/TiO_2/Si	800 nm/1.13×10^{-4} mW cm^{-2}	870

D* (Jones)	Response speed	Ref.
1.78×10^5	T_r=0.068 s	[16]
_	T_r=0.7 ms, T_d=0.8 ms	[17]
2.02×10^{13}	T_r=50.9 ms, T_d=26.0 ms	[18]
_	T_r=0.4 ms, T_d= 9 ms	[19]
6.2×10^{10}	T_r=0.04 ms, T_d=2.96 ms	[20]
6×10^{12}	T_r=116 ms, T_d=50 ms	[21]

References

[1] L. Qiao, X. Sun and R. Long, *J. Phys. Chem. Lett.,* 2019, **10**, 672.

[2] M. Ng and J. E. Halpert, *RSC Adv.,* 2020, **10**, 3832.

[3] N. Arora, M. I. Dar, M. Abdi-Jalebi, F. Giordano, N. Pellet, G. Jacopin, R. H. Friend, S. M. Zakeeruddin and M. Gratzel, *Nano Lett.,* 2016, **16**, 7155.

[4] S. Pachori, R. Agarwal, A. Shukla, U. Rani and A. S. Verma, *Int. J. Quantum Chem.,* 2021, **121**, e26671.

[5] T. Baikie, Y. Fang, J. M. Kadro, M. Schreyer, F. Wei, S. G. Mhaisalkar, M. Graetzel and T. J. White, *J. Mater. Chem. A,* 2013, **1**, 5628.

[6] L. Zhang, L. Liu, P. Zhang, R. Li, G. Zhang and X. Tao, *ACS Appl. Mater. Interfaces,* 2020, **12**, 39834.

[7] F. Babbe and C. M. Sutter-Fella, *Adv. Energy Mater.,* 2020, **10**, 1903587.

[8] A. Osherov, Y. Feldman, I. Kaplan-Ashiri, D. Cahen, G. Hodes and *Chem. Mater.,* 2020, **32**, 4223.

[9] Z. Yuan, W. Huang, S. Ma, G. Ouyang, W. Hu, W. Zhang and *J. Mater. Chem. C,* 2019, **7**, 5442.

[10] G. Yuan, S. Qin, X. Wu, H. Ding and A. Lu, *Phase Transitions,* 2017, **91**, 38.

[11] K. Wang, D. Yang, C. Wu, M. Sanghadasa and S. Priya, *Prog. Mater. Sci.,* 2019, **106**, 100580.

[12] S.Liu, A. R. DeFilippo, M. Balasubramanian, Z. Liu, S.G. Wang, Y.-S. Chen, S. Chariton, V. Prakapenka, X. Luo, L. Zhao, J. S. Martin, Y. Lin, Y. Yan, S. K. Ghose and T. A. Tyson, *Adv. Sci*., 2021, **8**, 2003046.

[13] P. Zhang, G. Zhang, L. Liu, D. Ju, L. Zhang, K. Cheng and X. Tao, *J. Phys. Chem. Lett.,* 2018, **9**, 5040.

[14] M. Naseri, D. M. Hoat, R. Ponce-Pérez, J. F. Rivas-Silva and G. H. Cocoletzi, *Chem. Phys.,* 2020, **531**, 110654.

[15] Q. Yao, J. Zhang, K. Wang, L. Jing, X. Cheng, C. Shang, J. Ding, W. Zhang, H. Sun and T. Zhou, *J. Mater. Chem. C,* 2021, **9**, 7374.

[16] J. Ding, H. Fang, Z. Lian, Q. Lv, J. L. Sun and Q. Yan, *Nanoscale,* 2018, **10**, 10538.

[17] M. Wang, W. Tian, F. Cao, M. Wang and L. Li, *Adv. Funct. Mater.,* 2020, **30**, 1909771.

[18] Y. Zou, T. Zou, C. Zhao, B. Wang, J. Xing, Z. Yu, J. Cheng, W. Xin, J. Yang, W. Yu, H. Dong and C. Guo, *Small,* 2020, **16**, 2000733.

[19] Z. Yang, Q. Xu, X. Wang, J. Lu, H. Wang, F. Li, L. Zhang, G. Hu and C. Pan, *Adv. Mater.,* 2018, **30**, 1802110.

[20] Y. Zhang, S. Li, W. Yang, M. K. Joshi and X. Fang, *J. Phys. Chem. Lett.,* 2019, **10**, 2400.

[21] F. Cao, Q. Liao, K. Deng, L. Chen, L. Li and Y. Zhang, *Nano Res.,* 2018, **11**, 1722.